ICES REPORT 18-01

January 2018

Convergence analysis of fixed stress split iterative scheme for anisotropic poroelasticity with tensor Biot parameter

by

Saumik Dana and Mary. F. Wheeler

The Institute for Computational Engineering and Sciences
The University of Texas at Austin
Austin, Texas 78712

Reference: Saumik Dana and Mary. F. Wheeler, "Convergence analysis of fixed stress split iterative scheme for anisotropic poroelasticity with tensor Biot parameter," ICES REPORT 18-01, The Institute for Computational Engineering and Sciences, The University of Texas at Austin, January 2018.

Convergence analysis of fixed stress split iterative scheme for anisotropic poroelasticity with tensor Biot parameter

Saumik Dana[a], Mary. F. Wheeler[a]

[a]*Center for Subsurface Modeling, Institute for Computational Engineering and Sciences, UT Austin, Austin, TX 78712*

Abstract

We perform a convergence analysis of the fixed stress split iterative algorithm for the Biot system modeling coupled flow and deformation in anisotropic poroelastic media with full Biot tensor. The fixed stress split iterative scheme solves the flow subproblem with all components of the stress tensor frozen using a multipoint flux mixed finite element method, followed by the poromechanics subproblem using a conforming Galerkin method in every coupling iteration at each time step. The coupling iterations are repeated until convergence and Backward Euler is employed for time marching. The convergence analysis is based on studying the equations satisfied by the difference of iterates to show that the fixed stress split iterative scheme for anisotropic poroelasticity with Biot tensor is contractive.

Keywords: Anisotropic poroelastic medium, Biot tensor, Fixed stress split iterative coupling, Contractivity

1. Introduction

Staggered solution algorithms are those in which operator splitting strategies are used to decompose coupled problems into subproblems which are then solved sequentially in successive iterations until a convergence criterion is met at each time step (Felippa et al. [13], Armero and Simo [3], Turska and Schrefler [25], Schrefler et al. [21]). The fixed stress split is one such operator splitting strategy for isotropic poroelasticity with scalar Biot parameter in which the flow problem is solved first while freezing the volumetric mean stress of the porous solid. Such an approach has been shown to enjoy numerical and theoretical convergence

Email addresses: saumik@utexas.edu (Saumik Dana), mfw@ices.utexas.edu (Mary. F. Wheeler)

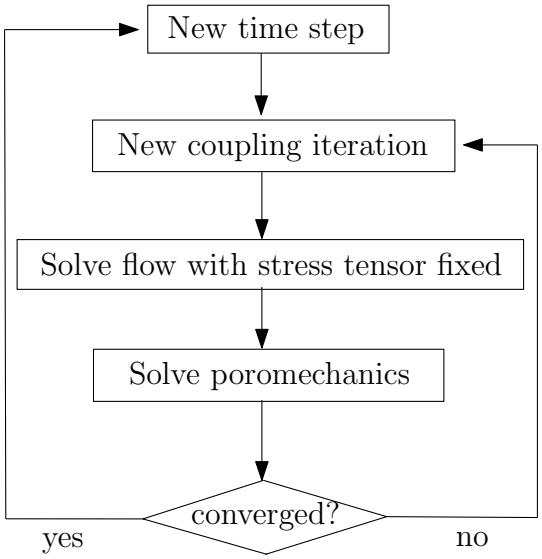

Figure 1: Fixed stress split iterative scheme for anisotropic poroelasticity with tensor Biot parameter

(Kim et al. [18], Mikelić and Wheeler [19], Castelletto et al. [10], Almani et al. [2]). The subject of this paper is the extension of the decoupling assumption to the case of anisotropic poroelasticity with tensor Biot parameter. The micromechanical analyses for the case of anisotropic poroelasticity (see Carroll [8], Carroll and Katsube [9], Katsube [17]) revealed that the modification to the stress applied to the porous solid due to the presence of pore fluid pressure is not hydrostatic, as it is in the case of isotropic poroelasticity (see Nur and Byerlee [20]). Further, unlike in case of isotropic poroelasticity where the solid-fluid coupling parameter is a scalar (see Biot [4], Geertsma [14], Skempton [23], Nur and Byerlee [20]), the coupling parameter in case of anisotropic poroelasticity is a tensor (see Biot [5], Coussy [12]). Intuitively, this implies that the decoupling assumption of freezing the hydrostatic part of the stress tensor during the flow solve in every coupling iteration for the case of isotropic poroelasticity requires a generalization for the case of anisotropic poroelasticity. As we shall show in the ensuing convergence analysis, the decoupling assumption of freezing all components of the stress tensor during the flow solve in every coupling iteration does enjoy theoretical convergence for the case of anisotropic poroelasticity with tensor Biot parameter. The convergence analysis is motivated by the previous work of Mikelić and Wheeler [19] and Almani et al. [2]. Mikelić and Wheeler [19] proved that the standard fixed stress split scheme for isotropic poroelasticity with scalar Biot parameter is a contraction

map with respect to appropriately chosen metrics. Almani et al. [2] extended those results to establish convergence of the multirate fixed stress split scheme in which the subproblems are resolved on different time scales with the poromechanics subproblem being resolved on a larger time scale. To the best of our knowledge, this is the first time a contraction map has been rigorously derived for the fixed stress split iterative scheme for anisotropic poroelasticity with tensor Biot parameter. This paper is structured as follows: Section 2 presents the model equations for flow and poromechanics. Section 3 presents the statement of contraction of the fixed stress split iterative scheme for anisotropic poroelasticity with tensor Biot parameter. Section 4 presents the convergence criterion for the algorithm.

1.1. Preliminaries

Given a bounded convex domain $\Omega \subset \mathbb{R}^3$, we use $P_k(\Omega)$ to represent the restriction of the space of polynomials of degree less that or equal to k to Ω and $Q_1(\Omega)$ to denote the space of trilinears on Ω. For the sake of convenience, we discard the differential in the integration of any scalar field χ over Ω as follows

$$\int_{\Omega} \chi(\mathbf{x}) \equiv \int_{\Omega} \chi(\mathbf{x})\, dV \qquad (\forall \mathbf{x} \in \Omega)$$

Sobolev spaces are based on the space of square integrable functions on Ω given by

$$L^2(\Omega) \equiv \big\{\theta : \|\theta\|_{\Omega}^2 := \int_{\Omega} |\theta|^2 < +\infty\big\},$$

The inner product of two second order tensors $\mathbf{S}$ and $\mathbf{T}$ is given by (see Gurtin et al. [15])

$$\mathbf{S} : \mathbf{T} = S_{ij} T_{ij} \qquad (i, j = 1, 2, 3)$$

A fourth order tensor is a linear transformation of a second order tensor to a second order tensor in the following manner (see Gurtin et al. [15])

$$\mathbb{P}\mathbf{S} = \mathbf{T} \rightarrow \mathbb{P}_{ijkl} S_{kl} = T_{ij} \qquad (i, j, k, l = 1, 2, 3)$$

2. Model equations

2.1. Flow model

Let the boundary $\partial\Omega = \Gamma_D^f \cup \Gamma_N^f$ where Γ_D^f is the Dirichlet boundary and Γ_N^f is the Neumann boundary. The fluid mass conservation equation (2.1) in the presence of deformable

and anisotropic porous medium with the Darcy law (2.2) and linear pressure dependence of density (2.3) with boundary conditions (2.4) and initial conditions (2.5) is

$$\frac{\partial \zeta}{\partial t} + \nabla \cdot \mathbf{z} = q \tag{2.1}$$

$$\mathbf{z} = -\frac{\mathbf{K}}{\mu}(\nabla p - \rho_0 \mathbf{g}) = -\boldsymbol{\kappa}(\nabla p - \rho_0 \mathbf{g}) \tag{2.2}$$

$$\rho = \rho_0(1 + c\,(p - p_0)) \tag{2.3}$$

$$p = g \text{ on } \Gamma_D^f \times (0,T],\ \mathbf{z} \cdot \mathbf{n} = 0 \text{ on } \Gamma_N^f \times (0,T] \tag{2.4}$$

$$p(\mathbf{x},0) = p_0(\mathbf{x}),\ \rho(\mathbf{x},0) = \rho_0(\mathbf{x}),\ \phi(\mathbf{x},0) = \phi_0(\mathbf{x}) \qquad (\forall \mathbf{x} \in \Omega) \tag{2.5}$$

where $p : \Omega \times (0,T] \to \mathbb{R}$ is the fluid pressure, $\mathbf{z} : \Omega \times (0,T] \to \mathbb{R}^3$ is the fluid flux, ζ is the fluid content, $\mathbf{n}$ is the unit outward normal on Γ_N^f, q is the source or sink term, $\mathbf{K}$ is the uniformly symmetric positive definite absolute permeability tensor, μ is the fluid viscosity, ρ_0 is a reference density, ϕ is the porosity, $\boldsymbol{\kappa} = \frac{\mathbf{K}}{\mu}$ is a measure of the hydraulic conductivity of the pore fluid, c is the fluid compressibility and $T > 0$ is the time interval.

2.2. Poromechanics model

Let the boundary $\partial\Omega = \Gamma_D^p \cup \Gamma_N^p$ where Γ_D^p is the Dirichlet boundary and Γ_N^p is the Neumann boundary. Linear momentum balance for the anisotropic porous solid in the quasi-static limit of interest (2.6) with small strain assumption (2.8) with boundary conditions (2.9) and initial condition (2.10) is

$$\nabla \cdot \boldsymbol{\sigma} + \mathbf{f} = \mathbf{0} \tag{2.6}$$

$$\mathbf{f} = \rho\phi\mathbf{g} + \rho_r(1-\phi)\mathbf{g} \tag{2.7}$$

$$\boldsymbol{\epsilon}(\mathbf{u}) = \frac{1}{2}(\nabla \mathbf{u} + (\nabla \mathbf{u})^T) \tag{2.8}$$

$$\mathbf{u} \cdot \mathbf{n}_1 = 0 \text{ on } \Gamma_D^p \times [0,T],\ \boldsymbol{\sigma}^T \mathbf{n}_2 = \mathbf{t} \text{ on } \Gamma_N^p \times [0,T] \tag{2.9}$$

$$\mathbf{u}(\mathbf{x},0) = \mathbf{0} \qquad \forall \mathbf{x} \in \Omega \tag{2.10}$$

where $\mathbf{u} : \Omega \times [0,T] \to \mathbb{R}^3$ is the solid displacement, ρ_r is the rock density, $\mathbf{f}$ is the body force per unit volume, $\mathbf{n}_1$ is the unit outward normal to Γ_D^p, $\mathbf{n}_2$ is the unit outward normal to Γ_N^p, $\mathbf{t}$ is the traction specified on Γ_N^p, $\boldsymbol{\epsilon}$ is the strain tensor, $\boldsymbol{\sigma}$ is the Cauchy stress tensor given by the generalized Hooke's law (see Coussy [12])

$$\boldsymbol{\sigma} = \boldsymbol{\sigma}_0 + \mathbb{M}\boldsymbol{\epsilon} - \boldsymbol{\alpha}(p - p_0) \tag{2.11}$$

where $\boldsymbol{\sigma}_0$ is the in situ stress, $\mathbb{M}$ is the fourth order anisotropic elasticity tensor and $\boldsymbol{\alpha}$ is the Biot tensor. The inverse of the generalized Hooke's law (2.11) is given by (see Cheng [11])

$$\boldsymbol{\epsilon} = \mathbb{C}\boldsymbol{\sigma} + \frac{1}{3}C\mathbf{B}p \tag{2.12}$$

where $\mathbb{C}$ is the fourth order anisotropic compliance tensor, $C(>0)$ is a generalized Hooke's law constant and $\mathbf{B}$ is a generalization of the Skempton pore pressure coefficient B (see Skempton [22]) for anisotropic poroelasticity.

2.3. Fluid content

The fluid content ζ is given by (see Cheng [11])

$$\zeta = Cp + \frac{1}{3}C\mathbf{B} : \boldsymbol{\sigma} \equiv \frac{1}{M}p + \boldsymbol{\alpha} : \boldsymbol{\epsilon} \tag{2.13}$$

where $M(>0)$ is a generalization of the Biot modulus (see Biot and Willis [6]) for anisotropic poroelasticity.

3. Statement of contraction of the fixed stress split scheme for anisotropic poroelasticity with Biot tensor

We use the notations $(\cdot)^{n+1}$ for any quantity $(\cdot)$ evaluated at time level $n+1$, $(\cdot)^{m,n+1}$ for any quantity $(\cdot)$ evaluated at the m^{th} coupling iteration at time level $n+1$, $\delta_f^{(m)}(\cdot)$ for the change in the quantity $(\cdot)$ during the flow solve over the $(m+1)^{th}$ coupling iteration at any time level and $\delta^{(m)}(\cdot)$ for the change in the quantity $(\cdot)$ over the $(m+1)^{th}$ coupling iteration at any time level. Let $\mathcal{T}_h$ be finite element partition of Ω consisting of distorted hexahedral elements E where $h = \max_{E\in\mathcal{T}_h} diam(E)$. The details of the finite element mapping are given in Appendix A. The discrete variational statements in terms of coupling iteration differences is : find $\delta^{(m)}p_h \in W_h$, $\delta^{(m)}\mathbf{z}_h \in \mathbf{V}_h$ and $\delta^{(m)}\mathbf{u}_h \in \mathbf{U}_h$ such that

$$C(\delta^{(m)}p_h, \theta_h)_\Omega + \Delta t(\nabla\cdot\delta^{(m)}\mathbf{z}_h, \theta_h)_\Omega = -\frac{C}{3}(\mathbf{B} : \delta^{(m-1)}\boldsymbol{\sigma}, \theta_h)_\Omega \tag{3.1}$$

$$(\boldsymbol{\kappa}^{-1}\delta^{(m)}\mathbf{z}_h, \mathbf{v}_h)_\Omega = (\delta^{(m)}p_h, \nabla\cdot\mathbf{v}_h)_\Omega \tag{3.2}$$

$$(\delta^{(m)}\boldsymbol{\sigma} : \boldsymbol{\epsilon}(\mathbf{q}_h))_\Omega = 0 \tag{3.3}$$

where the finite dimensional spaces W_h, $\mathbf{V}_h$ and $\mathbf{U}_h$ are

$$W_h = \left\{\theta_h : \theta_h| \in P_0(E)\ \forall E \in \mathscr{T}_h\right\}$$
$$\mathbf{V}_h = \left\{\mathbf{v}_h : \mathbf{v}_h|_E \leftrightarrow \hat{\mathbf{v}}|_{\hat{E}} \in \hat{\mathbf{V}}(\hat{E})\ \forall E \in \mathscr{T}_h,\ \mathbf{v}_h \cdot \mathbf{n} = 0 \text{ on } \Gamma_N^f\right\}$$
$$\mathbf{U}_h = \left\{\mathbf{q}_h = (u, v, w)|_E \in Q_1(E)\ \forall E \in \mathscr{T}_h,\ \mathbf{q}_h = \mathbf{0} \text{ on } \Gamma_D^p\right\}$$

and the details of $\hat{\mathbf{V}}(\hat{E})$ are given in Appendix B. The equations (3.1), (3.2) and (3.3) are the discrete variational statements (in terms of coupling iteration differences) of (2.1), (2.2) and (2.6) respectively. The details of (3.1) and (3.2) are given in Appendix C whereas the details of (3.3) are given in Appendix D.

Theorem 3.1. *The fixed stress split iterative coupling scheme for anisotropic poroelasticity with Biot tensor in which the flow problem is solved first by freezing all components of the stress tensor is a contraction given by*

$$\|\mathbf{B} : \delta^{(m)}\boldsymbol{\sigma}\|_\Omega^2 + \overbrace{2\|\delta^{(m)}p_h\|_\Omega^2}^{>0} + \overbrace{\frac{6\Delta t}{C}\|\boldsymbol{\kappa}^{-1/2}\delta^{(m)}\mathbf{z}_h\|_\Omega^2}^{>0} + \overbrace{\frac{6}{C}(\delta^{(m)}\boldsymbol{\sigma} : \mathbb{C}\delta^{(m)}\boldsymbol{\sigma})_\Omega}^{\geq 0} + \overbrace{\frac{3}{C^2}\|\delta^{(m)}\zeta\|_\Omega^2}^{>0}$$
$$- \frac{6}{C^2}\|\delta^{(m)}\zeta - \delta_f^{(m)}\zeta\|_\Omega^2 \leq \|\mathbf{B} : \delta^{(m-1)}\boldsymbol{\sigma}\|_\Omega^2$$

where the quantity $\|\delta^{(m)}\zeta - \delta_f^{(m)}\zeta\|_\Omega^2$ is driven to a small value via the convergence criterion for the algorithm.

Proof. • **Step 1: Flow equations**

Testing (3.1) with $\theta_h \equiv \delta^{(m)}p_h$, we get

$$C\|\delta^{(m)}p_h\|_\Omega^2 + \Delta t(\nabla \cdot \delta^{(m)}\mathbf{z}_h, \delta^{(m)}p_h)_\Omega = -\frac{C}{3}(\mathbf{B} : \delta^{(m-1)}\boldsymbol{\sigma}, \delta^{(m)}p_h)_\Omega \tag{3.4}$$

Testing (3.2) with $\mathbf{v}_h \equiv \delta^{(m)}\mathbf{z}_h$, we get

$$\|\boldsymbol{\kappa}^{-1/2}\delta^{(m)}\mathbf{z}_h\|_\Omega^2 = (\delta^{(m)}p_h, \nabla \cdot \delta^{(m)}\mathbf{z}_h)_\Omega \tag{3.5}$$

From (3.4) and (3.5), we get

$$C\|\delta^{(m)}p_h\|_\Omega^2 + \Delta t\|\boldsymbol{\kappa}^{-1/2}\delta^{(m)}\mathbf{z}_h\|_\Omega^2 = -\frac{C}{3}(\mathbf{B} : \delta^{(m-1)}\boldsymbol{\sigma}, \delta^{(m)}p_h)_\Omega \tag{3.6}$$

• **Step 2: Poromechanics equations**

Testing (3.3) with $\mathbf{q}_h \equiv \delta^{(m)}\mathbf{u}_h$, we get

$$(\delta^{(m)}\boldsymbol{\sigma} : \delta^{(m)}\boldsymbol{\epsilon})_\Omega = 0 \tag{3.7}$$

We now invoke (2.12) to arrive at the expression for change in strain tensor over the $(m+1)^{th}$ coupling iteration as follows

$$\delta^{(m)}\boldsymbol{\epsilon} = \mathbb{C}\delta^{(m)}\boldsymbol{\sigma} + \frac{C}{3}\mathbf{B}\delta^{(m)}p_h \tag{3.8}$$

Substituting (3.8) in (3.7), we get

$$(\delta^{(m)}\boldsymbol{\sigma} : \mathbb{C}\delta^{(m)}\boldsymbol{\sigma})_\Omega + \frac{C}{3}(\mathbf{B} : \delta^{(m)}\boldsymbol{\sigma}, \delta^{(m)}p_h)_\Omega = 0 \tag{3.9}$$

• Step 3: Combining flow and poromechanics equations

Adding (3.6) and (3.9), we get

$$\begin{aligned} &C\|\delta^{(m)}p_h\|_\Omega^2 + \Delta t\|\boldsymbol{\kappa}^{-1/2}\delta^{(m)}\mathbf{z}_h\|_\Omega^2 + (\delta^{(m)}\boldsymbol{\sigma} : \mathbb{C}\delta^{(m)}\boldsymbol{\sigma})_\Omega + \frac{C}{3}(\mathbf{B} : \delta^{(m)}\boldsymbol{\sigma}, \delta^{(m)}p_h)_\Omega \\ &= -\frac{C}{3}(\mathbf{B} : \delta^{(m-1)}\boldsymbol{\sigma}, \delta^{(m)}p_h)_\Omega \end{aligned} \tag{3.10}$$

• Step 4: Variation in fluid content

In lieu of (2.13), the variation in fluid content in the $(m+1)^{th}$ coupling iteration can be written as

$$\delta^{(m)}\zeta = C\delta^{(m)}p_h + \frac{C}{3}\mathbf{B} : \delta^{(m)}\boldsymbol{\sigma} \tag{3.11}$$

As a result, we can write

$$\frac{1}{2C}\|\delta^{(m)}\zeta\|_\Omega^2 - \frac{C}{2}\|\delta^{(m)}p_h\|_\Omega^2 - \frac{C}{18}\|\mathbf{B} : \delta^{(m)}\boldsymbol{\sigma}\|_\Omega^2 = \frac{C}{3}(\mathbf{B} : \delta^{(m)}\boldsymbol{\sigma}, \delta^{(m)}p_h)_\Omega \tag{3.12}$$

From (3.10) and (3.12), we get

$$\begin{aligned} &C\|\delta^{(m)}p_h\|_\Omega^2 + \Delta t\|\boldsymbol{\kappa}^{-1/2}\delta^{(m)}\mathbf{z}_h\|_\Omega^2 + (\delta^{(m)}\boldsymbol{\sigma} : \mathbb{C}\delta^{(m)}\boldsymbol{\sigma})_\Omega + \frac{1}{2C}\|\delta^{(m)}\zeta\|_\Omega^2 - \frac{C}{2}\|\delta^{(m)}p_h\|_\Omega^2 \\ &- \frac{C}{18}\|\mathbf{B} : \delta^{(m)}\boldsymbol{\sigma}\|_\Omega^2 = -\frac{C}{3}(\mathbf{B} : \delta^{(m-1)}\boldsymbol{\sigma}, \delta^{(m)}p_h)_\Omega \end{aligned} \tag{3.13}$$

Adding and subtracting $\frac{C}{6}\|\mathbf{B} : \delta^{(m)}\boldsymbol{\sigma}\|_\Omega^2$ to the LHS of (3.13) results in

$$\begin{aligned} &\frac{C}{6}\|\mathbf{B} : \delta^{(m)}\boldsymbol{\sigma}\|_\Omega^2 + \frac{C}{2}\|\delta^{(m)}p_h\|_\Omega^2 + \Delta t\|\boldsymbol{\kappa}^{-1/2}\delta^{(m)}\mathbf{z}_h\|_\Omega^2 + (\delta^{(m)}\boldsymbol{\sigma} : \mathbb{C}\delta^{(m)}\boldsymbol{\sigma})_\Omega + \frac{1}{2C}\|\delta^{(m)}\zeta\|_\Omega^2 \\ &- \frac{C}{9}\|\mathbf{B} : \delta^{(m)}\boldsymbol{\sigma}\|_\Omega^2 = -\frac{C}{3}(\mathbf{B} : \delta^{(m-1)}\boldsymbol{\sigma}, \delta^{(m)}p_h)_\Omega \end{aligned} \tag{3.14}$$

In lieu of (2.13) and the fixed stress constraint during the flow solve, the variation in fluid content during the flow solve in the $(m+1)^{th}$ coupling iteration is given by

$$\delta_f^{(m)}\zeta = C\delta_f^{(m)}p_h + \frac{C}{3}\mathbf{B} : \cancelto{\mathbf{0}}{\delta_f^{(m)}\boldsymbol{\sigma}}$$

Further, since the pore pressure is frozen during the poromechanical solve, we have $\delta_f^{(m)} p_h = \delta^{(m)} p_h$. As a result, we can write

$$\delta_f^{(m)} \zeta = C \delta^{(m)} p_h \tag{3.15}$$

Subtracting (3.15) from (3.11), we can write

$$\delta^{(m)} \zeta - \delta_f^{(m)} \zeta = \frac{C}{3} \mathbf{B} : \delta^{(m)} \boldsymbol{\sigma}$$

which implies that

$$\frac{1}{C} \| \delta^{(m)} \zeta - \delta_f^{(m)} \zeta \|_\Omega^2 = \frac{C}{9} \| \mathbf{B} : \delta^{(m)} \boldsymbol{\sigma} \|_\Omega^2 \tag{3.16}$$

In lieu of (3.16), we can write (3.14) as

$$\begin{aligned} &\frac{C}{6} \| \mathbf{B} : \delta^{(m)} \boldsymbol{\sigma} \|_\Omega^2 + \frac{C}{2} \| \delta^{(m)} p_h \|_\Omega^2 + \Delta t \| \boldsymbol{\kappa}^{-1/2} \delta^{(m)} \mathbf{z}_h \|_\Omega^2 + (\delta^{(m)} \boldsymbol{\sigma} : \mathbb{C} \delta^{(m)} \boldsymbol{\sigma})_\Omega + \frac{1}{2C} \| \delta^{(m)} \zeta \|_\Omega^2 \\ &- \frac{1}{C} \| \delta^{(m)} \zeta - \delta_f^{(m)} \zeta \|_\Omega^2 = -\frac{C}{3} (\mathbf{B} : \delta^{(m-1)} \boldsymbol{\sigma}, \delta^{(m)} p_h)_\Omega \end{aligned} \tag{3.17}$$

• Step 5: Invoking positive-semidefiniteness of the compliance tensor

The fourth order anisotropic compliance tensor $\mathbb{C}$ is positive-semidefinite (see Gurtin et al. [15]) in the sense that it obeys $\mathbf{S} : \mathbb{C}\mathbf{S} \geq 0$ for all symmetric tensors $\mathbf{S}$. In lieu of the above, since the Cauchy stress tensor is symmetric, the following holds true

$$\delta^{(m)} \boldsymbol{\sigma} : \mathbb{C} \delta^{(m)} \boldsymbol{\sigma} \geq 0 \tag{3.18}$$

In lieu of (3.18), we can write (3.17) as

$$\begin{aligned} &\frac{C}{6} \| \mathbf{B} : \delta^{(m)} \boldsymbol{\sigma} \|_\Omega^2 + \overbrace{\frac{C}{2} \| \delta^{(m)} p_h \|_\Omega^2}^{>0} + \overbrace{\Delta t \| \boldsymbol{\kappa}^{-1/2} \delta^{(m)} \mathbf{z}_h \|_\Omega^2}^{>0} + \overbrace{(\delta^{(m)} \boldsymbol{\sigma} : \mathbb{C} \delta^{(m)} \boldsymbol{\sigma})_\Omega}^{\geq 0} + \overbrace{\frac{1}{2C} \| \delta^{(m)} \zeta \|_\Omega^2}^{>0} \\ &- \frac{1}{C} \| \delta^{(m)} \zeta - \delta_f^{(m)} \zeta \|_\Omega^2 = -\frac{C}{3} (\mathbf{B} : \delta^{(m-1)} \boldsymbol{\sigma}, \delta^{(m)} p_h)_\Omega \end{aligned} \tag{3.19}$$

The quantity $\| \delta^{(m)} \zeta - \delta_f^{(m)} \zeta \|_\Omega^2$ on the LHS of (3.19) is driven to a small value via the convergence criterion for the algorithm as explained in Section 4.

• Step 6: Invoking the Young's inequality

Since the sum of the terms on the LHS of (3.19) is nonnegative, the RHS is also nonnegative. We invoke the Young's inequality (see Steele [24])

$$|ab| \leq \frac{a^2}{2} + \frac{b^2}{2} \qquad (\forall\ a, b \in \mathbb{R})$$

for the RHS of (3.19) as follows

$$-\frac{C}{3}(\mathbf{B}:\delta^{(m-1)}\boldsymbol{\sigma},\delta^{(m)}p_h)_\Omega \leq \frac{C}{3}\left(\frac{1}{2}\|\mathbf{B}:\delta^{(m-1)}\boldsymbol{\sigma}\|_\Omega^2+\frac{1}{2}\|\delta^{(m)}p_h\|_\Omega^2\right) \tag{3.20}$$

In lieu of (3.20), we write (3.19) as

$$\frac{C}{6}\|\mathbf{B}:\delta^{(m)}\boldsymbol{\sigma}\|_\Omega^2+\overbrace{\frac{C}{2}\|\delta^{(m)}p_h\|_\Omega^2}^{>0}+\overbrace{\Delta t\|\boldsymbol{\kappa}^{-1/2}\delta^{(m)}\mathbf{z}_h\|_\Omega^2}^{>0}+\overbrace{(\delta^{(m)}\boldsymbol{\sigma}:\mathbb{C}\delta^{(m)}\boldsymbol{\sigma})_\Omega}^{\geq 0}+\overbrace{\frac{1}{2C}\|\delta^{(m)}\zeta\|_\Omega^2}^{>0}$$
$$-\frac{1}{C}\|\delta^{(m)}\zeta-\delta_f^{(m)}\zeta\|_\Omega^2 \leq \frac{C}{6}\|\mathbf{B}:\delta^{(m-1)}\boldsymbol{\sigma}\|_\Omega^2+\frac{C}{6}\|\delta^{(m)}p_h\|_\Omega^2$$

which can also be written as

$$\|\mathbf{B}:\delta^{(m)}\boldsymbol{\sigma}\|_\Omega^2+\overbrace{2\|\delta^{(m)}p_h\|_\Omega^2}^{>0}+\overbrace{\frac{6\Delta t}{C}\|\boldsymbol{\kappa}^{-1/2}\delta^{(m)}\mathbf{z}_h\|_\Omega^2}^{>0}+\overbrace{\frac{6}{C}(\delta^{(m)}\boldsymbol{\sigma}:\mathbb{C}\delta^{(m)}\boldsymbol{\sigma})_\Omega}^{\geq 0}+\overbrace{\frac{3}{C^2}\|\delta^{(m)}\zeta\|_\Omega^2}^{>0}$$
$$-\frac{6}{C^2}\|\delta^{(m)}\zeta-\delta_f^{(m)}\zeta\|_\Omega^2 \leq \|\mathbf{B}:\delta^{(m-1)}\boldsymbol{\sigma}\|_\Omega^2 \tag{3.21}$$

□

4. Convergence criterion for the fixed stress split algorithm for anisotropic poroelasticity with Biot tensor

In lieu of (2.13), the variation in fluid content $\delta_f^{(m)}\zeta$ measured during the flow solve in the $(m+1)^{th}$ coupling iteration at any time step is

$$\delta_f^{(m)}\zeta=\frac{1}{M}\delta_f^{(m)}p_h+\boldsymbol{\alpha}:\delta_f^{(m)}\boldsymbol{\epsilon}=\zeta_p^{m+1}-\zeta^m \tag{4.1}$$

where ζ^m is the fluid content at the end of the previous or m^{th} coupling iteration and ζ_p^{m+1} serves as the predictor to the fluid content at the end of the current or $(m+1)^{th}$ coupling iteration. Similarly, the variation in fluid content $\delta^{(m)}\zeta$ over the $(m+1)^{th}$ coupling iteration (including the flow solve and poromechanics solve) at any time step is

$$\delta^{(m)}\zeta=\frac{1}{M}\delta^{(m)}p_h+\boldsymbol{\alpha}:\delta^{(m)}\boldsymbol{\epsilon}=\zeta_c^{m+1}-\zeta^m \tag{4.2}$$

where ζ_c^{m+1} serves as the corrector to ζ_p^{m+1}. Subtracting (4.1) from (4.2), we get

$$\delta^{(m)}\zeta-\delta_f^{(m)}\zeta\equiv\zeta_c^{m+1}-\zeta_p^{m+1}=\boldsymbol{\alpha}:(\delta^{(m)}\boldsymbol{\epsilon}-\delta_f^{(m)}\boldsymbol{\epsilon})=\boldsymbol{\alpha}:(\boldsymbol{\epsilon}_c^{m+1}-\boldsymbol{\epsilon}_p^{m+1})$$

which implies that the difference between the predicted value and the corrected value of the fluid content at the end of the $(m+1)^{th}$ coupling iteration is equal to the difference between the predicted value ($\boldsymbol{\epsilon}_p^{m+1}$) and the corrected value ($\boldsymbol{\epsilon}_c^{m+1}$) of the strain tensor at the end of the $(m+1)^{th}$ coupling iteration scaled by the Biot tensor $\boldsymbol{\alpha}$. In lieu of the above, the stopping criterion for coupling iterations at any time step is

$$\left\| \frac{\delta^{(m)}\zeta - \delta_f^{(m)}\zeta}{\zeta_c^{m+1}} \right\|_{L^\infty} \equiv \left\| \frac{\zeta_c^{m+1} - \zeta_p^{m+1}}{\zeta_c^{m+1}} \right\|_{L^\infty} \leq TOL$$

where $TOL > 0$ is a pre-specified tolerance.

Appendix A. Finite element mapping

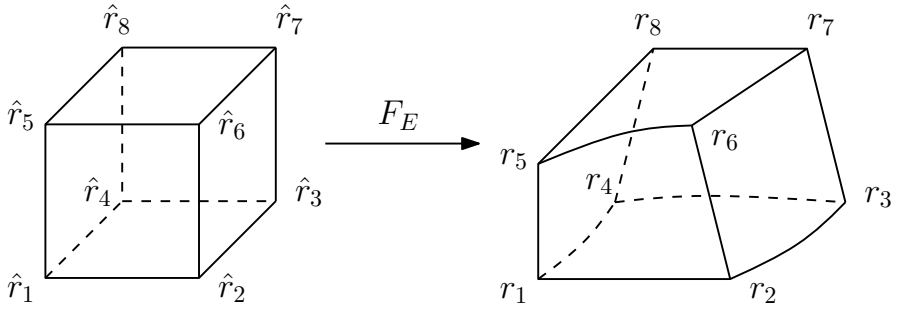

Figure A.2: Trilinear mapping $F_E : \hat{E} \to E$ for 8 noded distorted hexahedral elements. The faces of E can be non-planar.

Let $\mathbf{r}_i$, $i = 1, .., 8$ be the vertices of E. Now consider a reference cube $\hat{E}$ with vertices $\hat{\mathbf{r}}_1 = [0\ 0\ 0]^T$, $\hat{\mathbf{r}}_2 = [1\ 0\ 0]^T$, $\hat{\mathbf{r}}_3 = [1\ 1\ 0]^T$, $\hat{\mathbf{r}}_4 = [0\ 1\ 0]^T$, $\hat{\mathbf{r}}_5 = [0\ 0\ 1]^T$, $\hat{\mathbf{r}}_6 = [1\ 0\ 1]^T$, $\hat{\mathbf{r}}_7 = [1\ 1\ 1]^T$ and $\hat{\mathbf{r}}_8 = [0\ 1\ 1]^T$ as shown in Figure A.2. Let $\hat{\mathbf{x}} = (\hat{x}, \hat{y}, \hat{z}) \in \hat{E}$ and $\mathbf{x} = (x, y, z) \in E$. The function $F_E(\hat{\mathbf{x}}) : \hat{E} \to E$ is

$$\begin{aligned} F_E(\hat{\mathbf{x}}) = {} & \mathbf{r}_1(1-\hat{x})(1-\hat{y})(1-\hat{z}) + \mathbf{r}_2\hat{x}(1-\hat{y})(1-\hat{z}) + \mathbf{r}_3\hat{x}\hat{y}(1-\hat{z}) + \mathbf{r}_4(1-\hat{x})\hat{y}(1-\hat{z}) \\ & + \mathbf{r}_5(1-\hat{x})(1-\hat{y})\hat{z} + \mathbf{r}_6\hat{x}(1-\hat{y})\hat{z} + \mathbf{r}_7\hat{x}\hat{y}\hat{z} + \mathbf{r}_8(1-\hat{x})\hat{y}\hat{z} \end{aligned}$$

Denote Jacobian matrix by DF_E and let $J_E = det(DF_E)$. Defining $\mathbf{r}_{ij} \equiv \mathbf{r}_i - \mathbf{r}_j$, we have

$$DF_E(\hat{\mathbf{x}}) = \begin{bmatrix} \mathbf{r}_{21} + (\mathbf{r}_{34} - \mathbf{r}_{21})\hat{y} + (\mathbf{r}_{65} - \mathbf{r}_{21})\hat{z} + ((\mathbf{r}_{21} - \mathbf{r}_{34}) - (\mathbf{r}_{65} - \mathbf{r}_{78}))\hat{y}\hat{z}; \\ \mathbf{r}_{41} + (\mathbf{r}_{34} - \mathbf{r}_{21})\hat{x} + (\mathbf{r}_{85} - \mathbf{r}_{41})\hat{z} + ((\mathbf{r}_{21} - \mathbf{r}_{34}) - (\mathbf{r}_{65} - \mathbf{r}_{78}))\hat{x}\hat{z}; \\ \mathbf{r}_{51} + (\mathbf{r}_{65} - \mathbf{r}_{21})\hat{x} + (\mathbf{r}_{85} - \mathbf{r}_{41})\hat{y} + ((\mathbf{r}_{21} - \mathbf{r}_{34}) - (\mathbf{r}_{65} - \mathbf{r}_{78}))\hat{x}\hat{y} \end{bmatrix}$$

Denote inverse mapping by F_E^{-1}, its Jacobian matrix by DF_E^{-1} and let $J_{F_E^{-1}} = det(DF_E^{-1})$ such that

$$DF_E^{-1}(\mathbf{x}) = (DF_E)^{-1}(\hat{\mathbf{x}}); \qquad J_{F_E^{-1}}(\mathbf{x}) = (J_E)^{-1}(\hat{\mathbf{x}})$$

Let $\phi(\mathbf{x})$ be any function defined on E and $\hat{\phi}(\hat{\mathbf{x}})$ be its corresponding definition on $\hat{E}$. Then we have

$$\nabla\phi = (DF_E^{-1})^T(\mathbf{x})\,\hat{\nabla}\hat{\phi} = (DF_E)^{-T}(\hat{\mathbf{x}})\,\hat{\nabla}\hat{\phi} \tag{A.1}$$

Appendix B. Enhanced BDDF$_1$ spaces

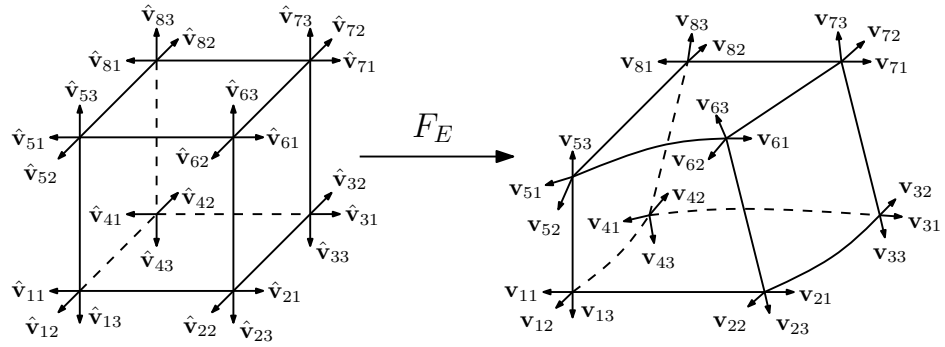

Figure B.3: Degrees of freedom and basis functions for the enhanced BDDF$_1$ velocity space on hexahedra.

For the sake of clarity, we provide a brief description of the mixed finite element spaces used in the flow model. Let $\mathbf{V}_h^* \times W_h$ be the lowest order BDDF$_1$ MFE spaces on hexahedra (see Brezzi et al. [7]). On the reference unit cube these spaces are defined as

$$\begin{aligned}\hat{\mathbf{V}}^*(\hat{E}) &= P_1(\hat{E}) + r_0\, curl(0,0,\hat{x}\hat{y}\hat{z})^T + r_1\, curl(0,0,\hat{x}\hat{y}^2)^T + s_0\, curl(\hat{x}\hat{y}\hat{z},0,0)^T \\ &\quad + s_1\, curl(\hat{y}\hat{z}^2,0,0)^T + t_0\, curl(0,\hat{x}\hat{y}\hat{z},0)^T + t_1\, curl(0,\hat{x}^2\hat{z},0)^T \\ \hat{W}(\hat{E}) &= \mathbb{P}_0(\hat{E})\end{aligned}$$

with the following properties

$$\hat{\nabla}\cdot\hat{\mathbf{V}}^*(\hat{E}) = \hat{W}(\hat{E}), \qquad \text{and} \qquad \forall\hat{\mathbf{v}} \in \hat{\mathbf{V}}^*(\hat{E}),\ \forall\hat{e} \subset \partial\hat{E},\ \hat{\mathbf{v}}\cdot\hat{\mathbf{n}}_{\hat{e}} \in P_1(\hat{e})$$

The multipoint flux approximation procedure requires on each face one velocity degree of freedom to be associated with each vertex. Since the BDDF$_1$ space $\mathbf{V}_h^*$ has only three

degrees of freedom per face, it is augmented with six more degrees of freedom (one extra degree of freedom per face). Since the constant divergence, the linear independence of the shape functions and the continuity of the normal component across the element faces are to be preserved, six curl terms are added (Ingram et al. [16]). Let $\mathbf{V}_h \times W_h$ be the enhanced BDDF_1 spaces on hexahedra. On the reference unit cube these spaces are

$$\begin{aligned}\hat{\mathbf{V}}(\hat{E}) &= \hat{\mathbf{V}}^*(\hat{E}) + r_2\, curl(0,0,\hat{x}^2\hat{z})^T + r_3\, curl(0,0,\hat{x}^2\hat{y}\hat{z})^T + s_2\, curl(\hat{x}\hat{y}^2,0,0)^T \\ &\quad + s_3\, curl(\hat{x}\hat{y}^2\hat{z}^2,0,0)^T + t_2\, curl(0,\hat{y}\hat{z}^2,0)^T + t_3\, curl(0,\hat{x}\hat{y}\hat{z}^2,0)^T \\ \hat{W}(\hat{E}) &= \mathbb{P}_0(\hat{E})\end{aligned}$$

with the following properties

$$\hat{\nabla}\cdot\hat{\mathbf{V}}(\hat{E}) = \hat{W}(\hat{E}), \qquad \text{and} \qquad \forall \hat{\mathbf{v}} \in \hat{\mathbf{V}}(\hat{E}),\ \forall \hat{e} \subset \partial\hat{E},\ \hat{\mathbf{v}}\cdot\hat{\mathbf{n}}_{\hat{e}} \in \mathbb{Q}_1(\hat{e})$$

where $\mathbb{Q}_1$ is the space of bilinear functions. Since $dim\,\mathbb{Q}_1(\hat{e}) = 4$, the dimension of $\hat{\mathbf{V}}(\hat{E})$ is 24 as shown in Figure B.3.

Appendix C. Discrete variational statements for the flow subproblem in terms of coupling iteration differences

Before arriving at the discrete variational statement of the flow model, we impose the fixed stress constraint on the strong form of the mass conservation equation (2.1). In lieu of (2.13), we write (2.1) as

$$\begin{aligned}&\frac{\partial}{\partial t}(Cp + \frac{C}{3}\mathbf{B}:\boldsymbol{\sigma}) + \nabla\cdot\mathbf{z} = q \\ &C\frac{\partial p}{\partial t} + \nabla\cdot\mathbf{z} = q - \frac{C}{3}\mathbf{B}:\frac{\partial\boldsymbol{\sigma}}{\partial t}\end{aligned} \tag{C.1}$$

Using backward Euler in time, the discrete in time form of (C.1) for the m^{th} coupling iteration in the $(n+1)^{th}$ time step is written as

$$C\frac{1}{\Delta t}(p^{m,n+1} - p^n) + \nabla\cdot\mathbf{z}^{m,n+1} = q^{n+1} - \frac{1}{\Delta t}\frac{C}{3}\mathbf{B}:(\boldsymbol{\sigma}^{m,n+1} - \boldsymbol{\sigma}^n)$$

where Δt is the time step and the source term as well as the terms evaluated at the previous time level n do not depend on the coupling iteration count as they are known quantities. The fixed stress constraint implies that $\boldsymbol{\sigma}^{m,n+1}$ gets replaced by $\boldsymbol{\sigma}^{m-1,n+1}$ i.e. the computation

of $p^{m,n+1}$ and $\mathbf{z}^{m,n+1}$ is based on the value of stress updated after the poromechanics solve from the previous coupling iteration $m-1$ at the current time level $n+1$. The modified equation is written as

$$C(p^{m,n+1}-p^n)+\Delta t\nabla\cdot\mathbf{z}^{m,n+1}=\Delta t q^{n+1}-\frac{C}{3}\mathbf{B}:(\boldsymbol{\sigma}^{m,n+1}-\boldsymbol{\sigma}^n)$$

As a result, the discrete weak form of (2.1) is given by

$$C(p_h^{m,n+1}-p_h^n,\theta_h)_\Omega+\Delta t(\nabla\cdot\mathbf{z}_h^{m,n+1},\theta_h)_\Omega=\Delta t(q^{n+1},\theta_h)_\Omega-\frac{C}{3}(\mathbf{B}:(\boldsymbol{\sigma}^{m-1,n+1}-\boldsymbol{\sigma}^n),\theta_h)_\Omega$$

Replacing m by $m+1$ and subtracting the two equations, we get

$$C(\delta^{(m)}p_h,\theta_h)_\Omega+\Delta t(\nabla\cdot\delta^{(m)}\mathbf{z}_h,\theta_h)_\Omega=-\frac{C}{3}(\mathbf{B}:\delta^{(m-1)}\boldsymbol{\sigma},\theta_h)_\Omega$$

The weak form of the Darcy law (2.2) for the m^{th} coupling iteration in the $(n+1)^{th}$ time step is given by

$$(\boldsymbol{\kappa}^{-1}\mathbf{z}^{m,n+1},\mathbf{v})_\Omega=-(\nabla p^{m,n+1},\mathbf{v})_\Omega+(\rho_0\mathbf{g},\mathbf{v})_\Omega\ \forall\ \mathbf{v}\in\mathbf{V}(\Omega)\tag{C.2}$$

where $\mathbf{V}(\Omega)$ is given by

$$\mathbf{V}(\Omega)\equiv\mathbf{H}(div,\Omega)\cap\left\{\mathbf{v}:\mathbf{v}\cdot\mathbf{n}=0\text{ on }\Gamma_N^f\right\}$$

and $\mathbf{H}(div,\Omega)$ is given by

$$\mathbf{H}(div,\Omega)\equiv\left\{\mathbf{v}:\mathbf{v}\in(L^2(\Omega))^3,\nabla\cdot\mathbf{v}\in L^2(\Omega)\right\}$$

We use the divergence theorem to evaluate the first term on RHS of (C.2) as follows

$$\begin{aligned}&(\nabla p^{m,n+1},\mathbf{v})_\Omega=(\nabla,p^{m,n+1}\mathbf{v})_\Omega-(p^{m,n+1},\nabla\cdot\mathbf{v})_\Omega\\&=(p^{m,n+1},\mathbf{v}\cdot\mathbf{n})_{\partial\Omega}-(p^{m,n+1},\nabla\cdot\mathbf{v})_\Omega=(g,\mathbf{v}\cdot\mathbf{n})_{\Gamma_D^f}-(p^{m,n+1},\nabla\cdot\mathbf{v})_\Omega\end{aligned}\tag{C.3}$$

where we invoke $\mathbf{v}\cdot\mathbf{n}=0$ on Γ_N^f. In lieu of (C.2) and (C.3), we get

$$(\boldsymbol{\kappa}^{-1}\mathbf{z}^{m,n+1},\mathbf{v})_\Omega=-(g,\mathbf{v}\cdot\mathbf{n})_{\Gamma_D^f}+(p^{m,n+1},\nabla\cdot\mathbf{v})_\Omega+(\rho_0\mathbf{g},\mathbf{v})_\Omega$$

Replacing m by $m+1$ and subtracting the two equations, we get

$$(\boldsymbol{\kappa}^{-1}\delta^{(m)}\mathbf{z}_h,\mathbf{v}_h)_\Omega=(\delta^{(m)}p_h,\nabla\cdot\mathbf{v}_h)_\Omega$$

Appendix D. Discrete variational statement for the poromechanics subproblem in terms of coupling iteration differences

The weak form of the linear momentum balance (2.6) is given by

$$(\nabla \cdot \boldsymbol{\sigma}, \mathbf{q})_\Omega + (\mathbf{f} \cdot \mathbf{q})_\Omega = 0 \qquad (\forall\ \mathbf{q} \in \mathbf{U}(\Omega)) \tag{D.1}$$

where $\mathbf{U}(\Omega)$ is given by

$$\mathbf{U}(\Omega) \equiv \big\{\mathbf{q} = (u, v, w) : u, v, w \in H^1(\Omega), \mathbf{q} = \mathbf{0} \text{ on } \Gamma_D^p\big\}$$

where $H^m(\Omega)$ is defined, in general, for any integer $m \geq 0$ as

$$H^m(\Omega) \equiv \big\{w : D^\alpha w \in L^2(\Omega)\ \forall |\alpha| \leq m\big\},$$

where the derivatives are taken in the sense of distributions and given by

$$D^\alpha w = \frac{\partial^{|\alpha|} w}{\partial x_1^{\alpha_1} .. \partial x_n^{\alpha_n}},\ |\alpha| = \alpha_1 + \cdots + \alpha_n,$$

We know from tensor calculus that

$$(\nabla \cdot \boldsymbol{\sigma}, \mathbf{q})_\Omega \equiv (\nabla, \boldsymbol{\sigma}\mathbf{q})_\Omega - (\boldsymbol{\sigma} : \nabla\mathbf{q})_\Omega \tag{D.2}$$

Further, using the divergence theorem and the symmetry of $\boldsymbol{\sigma}$, we arrive at

$$(\nabla, \boldsymbol{\sigma}\mathbf{q})_\Omega \equiv (\mathbf{q}, \boldsymbol{\sigma}\mathbf{n})_{\partial\Omega} \tag{D.3}$$

We decompose $\nabla\mathbf{q}$ into a symmetric part $(\nabla\mathbf{q})_s \equiv \frac{1}{2}\big(\nabla\mathbf{q} + (\nabla\mathbf{q})^T\big) \equiv \boldsymbol{\epsilon}(\mathbf{q})$ and skew-symmetric part $(\nabla\mathbf{q})_{ss}$ and note that the contraction between a symmetric and skew-symmetric tensor is zero to obtain

$$\boldsymbol{\sigma} : \nabla\mathbf{q} \equiv \boldsymbol{\sigma} : (\nabla\mathbf{q})_s + \cancelto{0}{\boldsymbol{\sigma} : (\nabla\mathbf{q})_{ss}} = \boldsymbol{\sigma} : \boldsymbol{\epsilon}(\mathbf{q}) \tag{D.4}$$

From (D.1), (D.2), (D.3) and (D.4), we get

$$(\boldsymbol{\sigma}\mathbf{n}, \mathbf{q})_{\partial\Omega} - (\boldsymbol{\sigma} : \boldsymbol{\epsilon}(\mathbf{q}))_\Omega + (\mathbf{f}, \mathbf{q})_\Omega = 0$$

which, after invoking the traction boundary condition, results in the discrete weak form for the m^{th} coupling iteration as

$$(\mathbf{t}^{n+1}, \mathbf{q}_h)_{\Gamma_N^p} - (\boldsymbol{\sigma}^{m,n+1} : \boldsymbol{\epsilon}(\mathbf{q}_h))_\Omega + (\mathbf{f}^{n+1}, \mathbf{q}_h)_\Omega = 0$$

Replacing m by $m+1$ and subtracting the two equations, we get

$$(\delta^{(m)}\boldsymbol{\sigma} : \boldsymbol{\epsilon}(\mathbf{q}_h))_\Omega = 0$$

References

[1] Y. Abousleiman, A. H. D. Cheng, L. Cui, E. Detournay, and J. C. Roegiers. Mandel's problem revisited. *Géotechnique*, 46(2):187–195, 1996.

[2] T. Almani, K. Kumar, A. Dogru, G. Singh, and M. F. Wheeler. Convergence analysis of multirate fixed-stress split iterative schemes for coupling flow with geomechanics. *Computer Methods in Applied Mechanics and Engineering*, 311:180–207, 2016.

[3] F. Armero and J. C. Simo. A new unconditionally stable fractional step method for non-linear coupled thermomechanical problems. *International Journal for Numerical Methods in Engineering*, 35(4):737–766, 1992.

[4] M. A. Biot. General theory of three dimensional consolidation. *Journal of Applied Physics*, 12:155–164, 1941.

[5] M. A. Biot. Theory of elasticity and consolidation for a porous anisotropic solid. *Journal of Applied Physics*, 26(2):182–185, 1955.

[6] M. A. Biot and D. G. Willis. The elastic coefficients of the theory of consolidation. *Journal of Applied Mechanics*, 24:594–601, 1957.

[7] F. Brezzi, J. Douglas, R. Durán, and M. Fortin. Mixed finite elements for second order elliptic problems in three variables. *Numerische Mathematik*, 51(2):237–250, 1987.

[8] M. M. Carroll. An effective stress law for anisotropic elastic deformation. *Journal of Geophysical Research*, 84(B13), 1979.

[9] M. M. Carroll and N. Katsube. The role of terzaghi effective stress in linearly elastic deformation. *Journal of Energy Resources Technology*, 105(4):509–511, 1983.

[10] N. Castelletto, J. A. White, and H. A. Tchelepi. Accuracy and convergence properties of the fixed-stress iterative solution of two-way coupled poromechanics. *International Journal for Numerical and Analytical Methods in Geomechanics*, 39(14):1593–1618, 2015.

[11] A. H. D. Cheng. Material coefficients of anisotropic poroelasticity. *International Journal of Rock Mechanics and Mining Sciences*, 34:199–205, 1997.

[12] O. Coussy. *Poromechanics*. Wiley, 2nd edition, 2004.

[13] C. A. Felippa, K. C. Park, and C. Farhat. Partitioned analysis of coupled mechanical systems. *Computer Methods in Applied Mechanics and Engineering*, 190(24):3247–3270, 2001.

[14] J. Geertsma. The effect of fluid pressure decline on volumetric changes of porous rocks. *SPE*, 210:331–340, 1957.

[15] M. E. Gurtin, E. Fried, and L. Anand. *The Mechanics and Thermodynamics of Continua*. Cambridge University Press, 1 edition, 2010.

[16] R. Ingram, M. F. Wheeler, and I. Yotov. A multipoint flux mixed finite element method on hexahedra. *SIAM Journal of Numerical Analysis*, 48(4):1281–1312, 2010.

[17] N. Katsube. The constitutive theory for fluid-filled porous materials. *Journal of Applied Mechanics*, 52(1):185–189, 1985.

[18] J. Kim, H. A. Tchelepi, and R. Juanes. Stability, accuracy and efficiency of sequential methods for coupled flow and geomechanics. *SPE Journal*, 16(2):249–262, 2011.

[19] A. Mikelić and M. F. Wheeler. Convergence of iterative coupling for coupled flow and geomechanics. *Computational Geosciences*, 17(3):455–461, 2013.

[20] A. Nur and J. D. Byerlee. An exact effective stress law for elastic deformation of rock with fluids. *Journal of Geophysical Research*, 76(26):6414–6419, 1971.

[21] B. A. Schrefler, L. Simoni, and E. Turska. Standard staggered and staggered newton schemes in thermo-hydro-mechanical problems. *Computer Methods in Applied Mechanics and Engineering*, 144(1-2):93–109, 1997.

[22] A. W. Skempton. The pore-pressure coefficients a and b. *Géotechnique*, 4(4):143–147, 1954.

[23] A. W. Skempton. Significance of terzaghi's concept of effective stress (terzaghi's discovery of effective stress). In *From theory to practice in soil mechanics (L. Bjerrum and A. Casagrande and R. B. Peek and A. W. Skempton, eds.). New York-London: John Wiley and Sons 1960*, 1960.

[24] J. M. Steele. *The Cauchy-Schwarz Master Class: An Introduction to the Art of Mathematical Inequalities*. Maa Problem Books Series. Cambridge University Press, 2004.

[25] E. Turska and B. A. Schrefler. On convergence conditions of partitioned solution procedures for consolidation problems. *Computer Methods in Applied Mechanics and Engineering*, 106(1-2):51–63, 1993.